The Effects of Correlated Noise in Intra-Complex DSN Arrays for S-Band Galileo Telemetry Reception

R. J. Dewey

Navigation Systems Section

A number of the proposals for supporting a Galileo S-band (2.3-GHz) mission involve arraying several antennas to maximize the signal-to-noise ratio (and bit rate) obtainable from a given set of antennas. Arraying is no longer a new idea, having been used successfully during the Voyager encounters with Uranus and Neptune. However, arraying for Galileo's tour of Jupiter is complicated by Jupiter's strong radio emission, which produces correlated noise effects. This article discusses the general problem of correlated noise due to a planet, or other radio source, and applies the results to the specific case of an array of antennas at the DSN's Tidbinbilla, Australia, complex (DSS 42, DSS 43, DSS 45, and the yet-to-be built DSS 34). The effects of correlated noise are highly dependent on the specific geometry of the array and on the spacecraft–planet configuration; in some cases, correlated noise effects produce an enhancement, rather than a degradation, of the signal-to-noise ratio. For the case considered here—an array of the DSN's Australian antennas observing Galileo and Jupiter—there are three regimes of interest. If the spacecraft–planet separation is $\lesssim 75$ arcsec, the average effect of correlated noise is a loss of signal to noise (~ 0.2 dB as the spacecraft–planet separation approaches zero). For spacecraft–planet separations $\gtrsim 75$ arcsec, but $\lesssim 400$ arcsec, the effects of correlated noise cause signal-to-noise variations as large as several tenths of a decibel over time scales of hours or changes in spacecraft–planet separation of tens of arcseconds; however, on average its effects are small (<0.01 dB). When the spacecraft is more than 400 arcsec from Jupiter (as is the case for about half of Galileo's tour), correlated noise is a <0.05-dB effect.

I. Introduction

It is now becoming common practice to array a number of antennas for telemetry reception in order to increase the effective aperture [1,2]. The signal-to-noise ratio (SNR) improvement obtained by arraying is straightforward to calculate when a pointlike spacecraft is the only source in the array's field of view. However, the calculation becomes complicated when an additional hot body (such as a radio-loud planet) is in the beam since, unlike system noise, the incoming radiation from this hot body is correlated at different antennas. This article presents a calculation

of the effect of correlated noise on the SNR achieved by a given array configuration. Other aspects of this topic have been discussed in [3] and in references therein.

This article is organized as follows: Sections II and III present a general formulation of the problem, Section IV considers the special case of an array of N identical antennas, and Section V looks at the specific case of arraying the DSN complex in Australia for Galileo S-band (2.3-GHz) telemetry reception. To make the article more readable, many of the detailed calculations have been relegated to the appendices. Much of the discussion parallels Hjellming's treatment of the Very Large Array (VLA) [4].

II. Outline of the Problem

Consider an array of N (not necessarily identical) antennas. The on-axis gain[1] of the ith antenna is denoted by G_i and its system temperature (looking at an empty field) is denoted by T_i. The direction toward a point on the sky can be described by a unit vector $\hat{s}$, with $\hat{s}_0$ pointing toward a source at the array's field center.[2] The shape of the ith antenna beam can be described by the field pattern,[3] a dimensionless function $f_i(\hat{s} - \hat{s}_0)$ such that $f_i^2(\hat{s} - \hat{s}_0)G_i$ describes the effective gain of the ith antenna in a direction $\hat{s} - \hat{s}_0$ from the beam center. In general, G_i, T_i, and f_i may all be elevation dependent. This dependence is not considered here; it can easily be included in quantitative calculations. The geometry of the array of N antennas can be described by the set of baseline vectors between each antenna pair $\mathbf{B}_{ik} = -\mathbf{B}_{ki}$, where $\mathbf{B}_{ik}$ denotes the vector from the ith antenna to the kth antenna. The basic geometry is shown in Fig. 1.

It is assumed that the spacecraft is transmitting a narrow-band, polarized signal with a total Earth-received power per unit area of $\mathcal{P}_{s/c}$ and that the planet has a total, unpolarized flux density (power per unit area per unit bandwidth) S_P. The angular distribution of the planet's radio emission is described by the brightness distribution

(flux density per unit solid angle) $I_P(\hat{s})$, which is assumed to be constant in time and only slowly varying with frequency (i.e., constant across the observing bandwidth).

Fairly simple assumptions are made about the method of arraying: The incoming RF signal at the ith antenna is mixed to baseband, after which a phase shift is inserted. This phase shift has a component ϕ_i^m (the model phase) that can be used to compensate, in real time, for phase differences between antennas (see Appendices A and C for details). The baseband signal is delayed by a model delay τ_i^m, and finally, the delayed signals from the N antennas are summed with appropriate weighting (see Appendix D). It is assumed that the signal is filtered through a rectangular baseband filter of width $\Delta\nu$; for an upper sideband system (which is assumed throughout), the sky frequency at the center of the passband is $\nu_{sky}^c = \nu_{lo} + \Delta\nu/2$, where ν_{lo} is the mixer frequency. It is also assumed that the model delays are chosen so as to compensate for the delay that a signal from the direction $\hat{s}_0$ (the field center) suffers between an arbitrary reference point and the ith antenna.

$$\tau_i^m = \frac{\mathbf{r}_i \cdot \hat{s}_0}{c} \tag{1}$$

where $\mathbf{r}_i$ is the vector from the reference point to antenna i. A simple block diagram of the signal path is shown in Fig. 2.

The total arrayed power can be written as the sum of the arrayed power from each of the three sources $P_\Sigma = P_\Sigma^{s/c} + P_\Sigma^P + P_\Sigma^N$, where $P_\Sigma^{s/c}, P_\Sigma^P, P_\Sigma^N$, represent, respectively, the arrayed power from the spacecraft, from the planet, and from system noise.[4] The effective SNR of the array is proportional to the ratio of the arrayed spacecraft power to the total arrayed power; in the low signal limit, this reduces to the ratio of $P_\Sigma^{s/c}$ to the power received from all sources other than the spacecraft (in this case, the planet and system noise). A figure of merit β can be defined for an array; β is analogous to G/T for a single dish and quantifies how, for a given spacecraft power $(\mathcal{P}_{s/c})$ an observing bandwidth $(\Delta\nu)$, the SNR varies with the following array configuration:

$$\beta = \frac{\Delta\nu}{2\mathcal{P}_{s/c}} \frac{P_\Sigma^{s/c}}{P_\Sigma} \approx \frac{\Delta\nu}{2\mathcal{P}_{s/c}} \frac{P_\Sigma^{s/c}}{P_\Sigma^P + P_\Sigma^N} \tag{2}$$

---

[1] Throughout this article, an astronomer's definition of antenna gain is used (commonly measured in units of K per Jy) of $G = \epsilon A/2k_B$, where ϵ is the dimensionless antenna efficiency, A is the physical antenna area, and k_B is Boltzmann's constant.

[2] Here, $\hat{s}_0$ is defined as the nominal direction in which the antennas in the array are pointing, which is the direction assumed when model delays are calculated (see Appendix A). As discussed in Appendix C, it is not necessarily the phase center of the array.

[3] In general, the field pattern is considered to be a complex quantity (e.g., [5, p. 27]), but for the purposes of this article, it is sufficient to assume that it is real.

[4] System noise includes receiver noise, sky background, and ground pickup—all sources of unwanted noise other than individual, identifiable sources (such as a planet) in the field of view.

The term $P_\Sigma^{s/c}/P_\Sigma$ is the SNR; the term $\Delta\nu/2\ P_\Sigma^{s/c}$ is a normalization factor that removes from β any dependence on quantities other than array and source geometry.

III. General Expression for β

As discussed in Appendix A, the summed baseband voltage can be written in the form

$$v_\Sigma(\nu, t) = \sum_{i=1}^{N} W_i e^{-i\phi_i^m} v_i(\nu, t + \tau_i^m) \qquad (3)$$

where $v_i(\nu, t)$ is the baseband voltage given by Eq. (A-4), ν is the baseband frequency, and W_i is the weighting factor.

The arrayed power is then

$$P_\Sigma = \left\langle \int_0^{\Delta\nu} d\nu\ |v_\Sigma(\nu, t)|^2 \right\rangle_T$$

$$= \left\langle \int_0^{\Delta\nu} d\nu \left| \sum_{i=1}^{N} W_i e^{-i\phi_i^m} v_i(\nu, t + \tau_i^m) \right|^2 \right\rangle_T$$

$$= \sum_{i=1}^{N} W_i^2 P_i + \sum_{i=1}^{N}\sum_{k \neq i}^{N} W_i W_k \rho_{ik} \qquad (4)$$

where the angle brackets denote time averaging and T is the interval over which the time average is taken; P_i is the single dish power from the ith antenna,

$$P_i = \left\langle \int_0^{\Delta\nu} d\nu\ |v_i(\nu, t)|^2 \right\rangle_T \qquad (5)$$

and ρ_{ik} is the unnormalized correlation between the ith and kth antennas,

$$\rho_{ik} = \left\langle \int_0^{\Delta\nu} d\nu\ e^{i(\phi_k^m - \phi_i^m)} v_i(\nu, t + \tau_i^m) v_k^*(\nu, t + \tau_k^m) \right\rangle_T \qquad (6)$$

As can be seen in Eqs. (A-11) and (A-18), both P_i and ρ_{ik} can be written as the sum of contributions from the

spacecraft $(P_i^{s/c}, \rho_{ik}^{s/c})$, the planet (P_i^P, ρ_{ik}^P), and random noise (P_i^N, ρ_{ik}^N), so Eq. (4) can be written

$$P_\Sigma = \sum_{i=1}^{N} W_i^2 (P_i^{s/c} + P_i^P + P_i^N)$$

$$+ \sum_{i=1}^{N}\sum_{k \neq i}^{N} W_i W_k (\rho_{ik}^{s/c} + \rho_{ik}^P + \rho_{ik}^N) \qquad (7)$$

Thus, P_Σ, the total power in the arrayed signal, can be written as the sum of contributions from the three sources (the spacecraft, the planet, and system noise), $P_\Sigma = P_\Sigma^{s/c} + P_\Sigma^P + P_\Sigma^N$, with

$$P_\Sigma^{s/c} = \sum_{i=1}^{N} W_i^2 P_i^{s/c} + \sum_{i=1}^{N}\sum_{k \neq i}^{N} W_i W_k \rho_{ik}^{s/c} \qquad (8)$$

$$P_\Sigma^P = \sum_{i=1}^{N} W_i^2 P_i^P + \sum_{i=1}^{N}\sum_{k \neq i}^{N} W_i W_k \rho_{ik}^P \qquad (9)$$

$$P_\Sigma^N = \sum_{i=1}^{N} W_i^2 P_i^N + \sum_{i=1}^{N}\sum_{k \neq i}^{N} W_i W_k \rho_{ik}^N$$

$$\approx \sum_{i=1}^{N} W_i^2 P_i^N \qquad (10)$$

Because the phases of the individual ρ_{ik}^N terms in Eq. (10) are random, their sum is always small (on average, zero) and was dropped. However, the sums over ρ_{ik}^P and $\rho_{ik}^{s/c}$ are not necessarily small; in fact, a key aspect of arraying is choosing the inserted model phases to ensure that the sum over $\rho_{ik}^{s/c}$ is maximized (see Appendix C). Expressions for $P_i^{s/c}$, P_i^P, and P_i^N are derived in Appendix A, Section II, and given by Eqs. (A-13), (A-14), and (A-15), respectively. Expressions for $\rho_{ik}^{s/c}$ and ρ_{ik}^P are derived in Appendix A, Section C, and given by Eqs. (A-25) and (A-28). Substituting Eqs. (8)–(10) into Eq. (2) gives

$$\beta = \frac{\Delta\nu}{2P_{s/c}} \times \frac{\displaystyle\sum_{i=1}^{N} W_i^2 P_i^{s/c} + \sum_{i=1}^{N}\sum_{k \neq i}^{N} W_i W_k \rho_{ik}^{s/c}}{\displaystyle\sum_{i=1}^{N} W_i^2 (P_i^N + P_i^P) + \sum_{i=1}^{N}\sum_{k \neq i}^{N} W_i W_k \rho_{ik}^P} \qquad (11)$$

The phases of $\rho_{ik}^{s/c}$ and ρ_{ik}^P depend on the quantity $\delta\phi_i - \delta\phi_k = \phi_i - \phi_i^m - \phi_k + \phi_k^m$, where ϕ_i, ϕ_k are the actual antenna-based phases, which include both hardware and atmospheric effects, and ϕ_i^m, ϕ_k^m are the model phases. If no attempt is made to compensate for the individual antenna phases (i.e., if $\phi_i^m = \phi_k^m = 0$), the phases of $\rho_{ik}^{s/c}$ and ρ_{ik}^P are uncorrelated from baseline to baseline, and in both Eqs. (8) and (9) the sums over the cross-correlation will be small (zero on average). However, as discussed in Appendix C, the total phase of $\rho_{ik}^{s/c}$ will be zero for all i, k, if the values of ϕ_i^m, ϕ_k^m are chosen to satisfy Eq. (C-1):

$$\delta\phi_i - \delta\phi_k = \phi_i - \phi_i^m - \phi_k + \phi_k^m$$

$$= -2\pi\nu^{s/c}\frac{\mathbf{B}_{ik}}{c}\cdot[\hat{\mathbf{s}}_{s/c} - \hat{\mathbf{s}}_0]$$

When ϕ_i^m, ϕ_k^m are chosen to satisfy the above expression, all the terms in the double sum in Eq. (8) add in phase, and for large N, the sum over $\rho_{ik}^{s/c}$ contributes significantly more to $P_\Sigma^{s/c}$ than does the sum over $P_i^{s/c}$ (since $\rho_{ik} \sim \sqrt{P_iP_k}$). Phases chosen to satisfy Eq. (C-1) maximize $P_\Sigma^{s/c}$, and except in pathological[5] cases this choice maximizes β. The process of determining and inserting these values of ϕ_i^m, ϕ_k^m is referred to as phasing the array. In the following, the subscript ϕ is used to denote expressions that assume that the array is phased on the spacecraft.

Unfortunately, the values of ϕ_i^m, ϕ_k^m, which maximize the sum over $\rho_{ik}^{s/c}$, may also de-randomize the phases of ρ_{ik}^P; as a consequence, sums over ρ_{ik}^P in Eqs. (4) and (11)

can become significantly nonzero. This is the source of the correlated noise contribution from the planet.

Equations (A-13), (A-14), (A-15), (A-25), and (A-28) can be used to expand Eqs. (8), (9), and (10), and if the array is phased on the spacecraft [Eq. (C-1) is satisfied], the arrayed power from the spacecraft, the planet, and system noise can be written, respectively, as

$$P_{\Sigma\phi}^{s/c} = 2k_B\mathcal{P}_{s/c}\left[\sum_{i=1}^{N}W_i^2G_i + \sum_{i=1}^{N}\sum_{k\neq i}^{N}W_iW_k\sqrt{G_iG_k}\right] \quad (12)$$

$$P_{\Sigma\phi}^P = \Delta\nu k_B S_P\left[\sum_{i=1}^{N}W_i^2\bar{f}_{i_P}^2 G_i \right.$$

$$\left. + \sum_{i=1}^{N}\sum_{k\neq i}^{N}W_iW_k\bar{f}_{i_P}\bar{f}_{k_P}\sqrt{G_iG_k}\,\mathcal{F}_{ik}^P\right] \quad (13)$$

$$P_{\Sigma\phi}^N = \Delta\nu k_B\sum_{i=1}^{N}W_i^2T_i \quad (14)$$

In the above expressions, $\bar{f}_{i_P}$, $\bar{f}_{k_P}$ represent the average value of the beam pattern in the direction of the planet, and $\mathcal{F}_{ik}^P$ [defined by Eq. (A-27)] is a dimensionless, complex quantity, with magnitude less than or equal to unity, which depends only on the array geometry and the structure of the planet (or other background source).

By inserting Eqs. (12), (13), and (14) into Eq. (2), the expression for β reduces to

$$\beta_\phi = \frac{\left[\sum_{i=1}^{N}W_i^2G_i + \sum_{i=1}^{N}\sum_{k\neq i}^{N}W_iW_k\sqrt{G_iG_k}\right]}{S_P\left[\sum_{i=1}^{N}W_i^2\bar{f}_{i_P}^2 G_i + \sum_{i=1}^{N}\sum_{k\neq i}^{N}W_iW_k\bar{f}_{i_P}\bar{f}_{k_P}\sqrt{G_iG_k}\,\mathcal{F}_{ik}^P\right] + \sum_{i=1}^{N}W_i^2T_i} \quad (15)$$

IV. An Array of Identical Antennas

The major effects of correlated noise are easily seen by examining an array of identical antennas. Consider an array of N antennas, each with a gain G, a system temperature T, and an average field pattern in the direction of the planet $\bar{f}_P$. Since the antennas are identical, $W_i = 1$ for all

---

[5] One can imagine cases where the increase in $P_\Sigma^{s/c}$ obtained by phasing the array is more than counteracted by the resulting increase in P_Σ^P, but even attempting to array in such cases would be difficult.

i. When this array is properly phased on the spacecraft, Eqs. (12), (13), and (14) become

$$P^{s/c}_{\Sigma\phi} = 2k_B N^2 G P_{s/c} \qquad (16)$$

$$P^P_{\Sigma\phi} = \Delta\nu k_B \bar{f}^2_P G S_P \left[N + \sum_{i=1}^{N} \sum_{k\neq i}^{N} \mathcal{F}^P_{ik} \right] \qquad (17)$$

$$P^N_{\Sigma\phi} = \Delta\nu k_B N T \qquad (18)$$

and Eq. (15) becomes

$$\beta_\phi = \frac{NG}{\bar{f}^2_P G S_P \left[1 + N^{-1} \sum\limits_{i=1}^{N} \sum\limits_{k\neq i}^{N} \mathcal{F}^P_{ik} \right] + T} \qquad (19)$$

Since $|\mathcal{F}^P_{ik}| \leq 1$ for all baselines, it is always true that

$$1 + N^{-1} \sum_{i=1}^{N} \sum_{k\neq i}^{N} \mathcal{F}^P_{ik} \leq N \qquad (20)$$

From Eq. (A-27) [see also Eqs. (B-1), (B-3), and (B-5)], it can be seen that, in the limit of an extremely compact array [i.e., $B_{ik} \ll c/(\nu^c_{sky} R_P)$, for all i, k; R_P being the characteristic angular radius of the planet], $\mathcal{F}^P_{ik} \to 1$ on all baselines and

$$\beta_{\phi_0} \to \frac{NG}{NGS_P + T} \qquad (21)$$

where the substitution $\bar{f}_P = 1$, appropriate in this limit,[6] has been made. This is equivalent to observing the spacecraft with a single dish of gain NG and an effective system temperature of NGS_P+T. Not surprisingly, observing the spacecraft and planet with a compact array is analogous to observing the two objects with an antenna with N times the area of a single array element.

In the limit where $B_{ik} \gg c/(\nu^c_{sky} R_P)$, for all i, k (i.e., an extremely extended array), $|\mathcal{F}^P_{ik}| \to 0$ on all baselines and

---

[6] If the baseline is small compared to $c/(\nu^c_{sky} R_P)$, the diameters of the individual antennas would be smaller still.

$$\beta_{\phi_\infty} \to \frac{NG}{\bar{f}^2_P G S_P + T} \qquad (22)$$

This is equivalent to observing the spacecraft with a single dish of gain NG and an effective system temperature of $\bar{f}^2_P G S_P + T$.

In both cases, the effective gain is NG; it is independent of baseline length and depends only on the gains of the individual antennas. However, the effective system temperature is not the same in the two extreme configurations. The planet contributes $N\bar{f}^2_P G S_P$ to the system temperature in the compact array limit but only $\bar{f}^2_P G S_P$ in the extended array limit. In the extended array limit, the noise contribution from the planet is simply the sum of its (uncorrelated) contributions to the individual system temperature. In the compact array limit, its contribution is N times larger due to the correlated noise effects.

Though, as discussed below, the effects of correlated noise are a complicated function of array geometry. In general, *the more extended the array configuration, the smaller the correlated noise contribution* of a planet or other hot body. As a rule of thumb, correlated-noise contributions are significant on baselines where $\nu^c_{sky} B_{ik} R_P/c \lesssim 1$ (see Appendix A, Section III).

It should be noted that in the intermediate cases where $B_{ik} \sim C/(\nu^c_{sky} R_P)$, the sum over $\mathcal{F}^P_{ik}$ may, for some geometries, be negative. In such cases, the performance of the array is actually enhanced over that of the extended array limit.

V. DSN Complexes at S-Band

One of the proposals for support of the Galileo S-band mission is the arraying of antennas at each DSN complex. This section describes the performance of an array at the Canberra complex that includes DSS 42, 43, 45, and the soon-to-be-built DSS 34. Table 1 lists each antenna, its S-band gain and system temperature at zenith, its S-band beamwidth at full-width half-power (FWHP), and its station coordinates (east, north, and vertical) relative to DSS 43.

With the model of Jupiter given in Appendix B, Eq. (15) can be used to calculate β_ϕ for the array. The improvement that the array would provide relative to the stand-alone use of DSS 43, if correlated noise effects could be neglected, is given by the ratio

$$\frac{\beta_{\phi_\infty}}{\beta_{43}} = \frac{\left[\sum_{i=1}^{N} W_i^2 G_i + \sum_{i=1}^{N} \sum_{k \neq i}^{N} W_i W_k \sqrt{G_i G_k}\right]}{S_P \sum_{i=1}^{N} W_i^2 f_{i_P}^2 G_i + \sum_{i=1}^{N} W_i^2 T_i}$$

$$\times \frac{T_{43} + f_{43_P}^2 G_{43} S_P}{G_{43}} \qquad (23)$$

When correlated noise is neglected, this ratio is independent of hour angle, array geometry, or source structure, but it depends on S_P—the flux of Jupiter—and, therefore, on the Earth–Jupiter distance. At opposition, this distance is 4.2 AU, the S-band flux of Jupiter is approximately 5.8 Jy and, with the parameters given in Table 1, $\beta_{\phi_\infty}/\beta_{43} = 1.41$. At conjunction (an Earth–Jupiter distance of 6.2 AU), $S_P \approx 2.6$ Jy and $\beta_{\phi_\infty}/\beta_{43} = 1.38$. The improvement is not as great at large Earth–Jupiter distances because Jupiter's contribution to the system temperature is less; for comparison, if $S_P = 0$, $\beta_{\phi_\infty}/\beta_{43} = 1.34$. It is useful to note that despite the effects of correlated noise, arraying is most useful when extended background sources are present, particularly if the baselines are long. In the above calculations, it is assumed that $\bar{f}_P = 1$ for all antennas and, as in all the calculations in this section, $W_i = \sqrt{G_i}/T_i$ [see Eq. (D-4)]. Throughout this section, it is also assumed that the gains G_i and system temperatures T_i do not vary with elevation, which leads to a slight overestimate of correlated noise effects at low elevations.

To assess the effects of correlated noise, the SNR provided by the actual array is compared with that provided by the same antennas if arrayed in a configuration with infinitely long baselines, examining the ratio $\beta_\phi/\beta_{\phi_\infty}$. This ratio depends not only on Earth–Jupiter distance, but, in a complicated way, on the array and source geometries and on hour angle. Figure 3 plots this ratio for a number of different geometries. In each plot the declination of Jupiter,[7] the Earth–Jupiter distance, and the angular sep-

aration between the spacecraft and the center of Jupiter are held fixed. Each point on the plot then represents the value of $\beta_\phi/\beta_{\phi_\infty}$ for a randomly chosen value of the hour angle, the orientation on the sky of Jupiter's radiation belts, and the orientation of the spacecraft–Jupiter separation. Thus, the density of points on a portion of a plot provides an estimate of the likelihood, as a function of the hour angle, of obtaining a particular value of $\beta_\phi/\beta_{\phi_\infty}$ for the given parameters.

Figures 4(a) and (b) summarize the results of the calculations shown in Fig. 3 plotting, as a function of spacecraft–Jupiter separation, the average (over hour angle and orientation) value of $\beta_\phi/\beta_{\phi_\infty}$, as well as its minimum and maximum values. Thus, each plot in Fig. 3 is reduced to three points in Fig. 4—one on an average curve, one on a maximum curve, and one on a minimum curve. The following conclusions can be drawn from Fig. 4:

(1) When Galileo is within ~75 arcsec of Jupiter, the average effect of correlated noise is a loss of SNR, which may be as large as 5 percent at zero separation.

(2) When Galileo is more than 400 arcsec from Jupiter, the effects of correlated noise are negligible.

(3) For separations in the range of 75 to 400 arcsec, the effects of correlated noise are small *on average*. However, the loss may be significant for certain geometries (as may be the enhancement). In this range of planet–spacecraft separations, careful calculations of correlated noise are necessary in a case where a 5-percent SNR loss would be critical.

The above conclusions refer specifically to an array consisting of the antennas listed in Table 1. Correlated noise effects are likely to be similar for arrays of similar antennas with similar baseline geometries, but quantitative calculations for other arrays have not been carried out. Because correlated noise causes significant SNR variations, and because these variations are highly geometry dependent, detailed calculations of these effects should be done for any situations in which a few tenths of a decibel of SNR are crucial. For most purposes involving Galileo and Jupiter, Eqs. (15), (B-6), and (B-9) should be suitable for such calculations.

---

[7] A declination of -21 deg, corresponding to that of the Galileo encounter in December 1995, has been used for Fig. 3. The results for other Jupiter declinations are different in detail but qualitatively very similar.

Acknowledgments

Table 1. S-band parameters of antennas in proposed Canberra array.

Antenna	Gain, K/Jy	System temperature, K	S-band beamwidth (FWHM), deg	Station coordinates[a]		
				East, m	North, m	Vertical, m
DSS 43	0.95	18.5	0.11	0.0	0.0	0.0
DSS 42	0.21	22.0	0.28	0.0003	194.1921	−13.6414
DSS 45	0.16	38.0	0.23	−325.3907	440.1822	−13.1378
DSS 34[b]	0.16	30.0	0.23	68.8	440.2	0.0

[a] Relative to DSS 43.

[b] Values for DSS 34 are approximate.
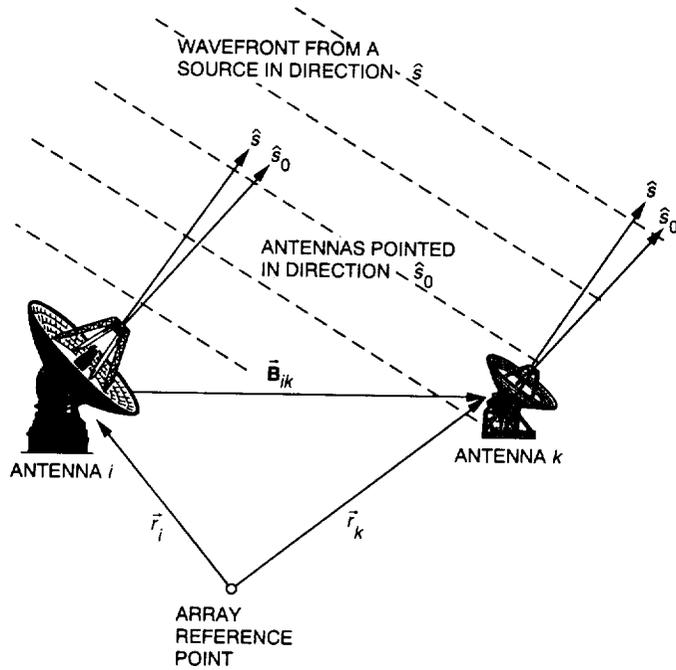
Fig. 1. The basic geometry of an array. Antennas i and k are located at, respectively, r_i and r_k with respect to the array reference point and are pointed toward the direction $\hat{s}_0$. It is clear from the diagram that the delay suffered by a wavefront from a direction $\hat{s}$ between antenna i and antenna k is proportional to $B_{ik} \cdot \hat{s}$.
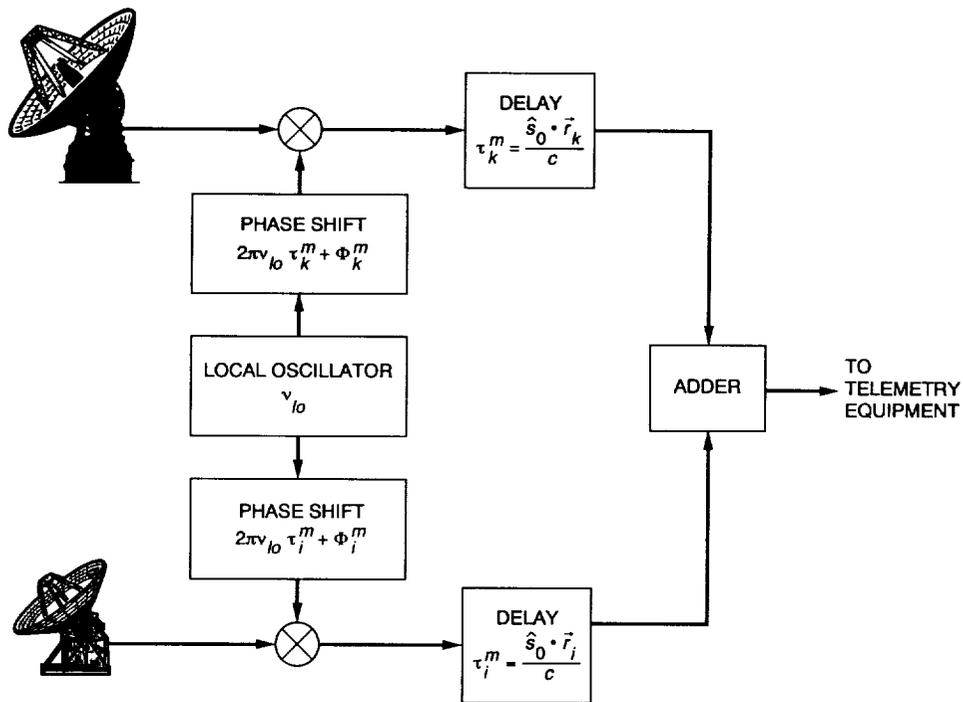
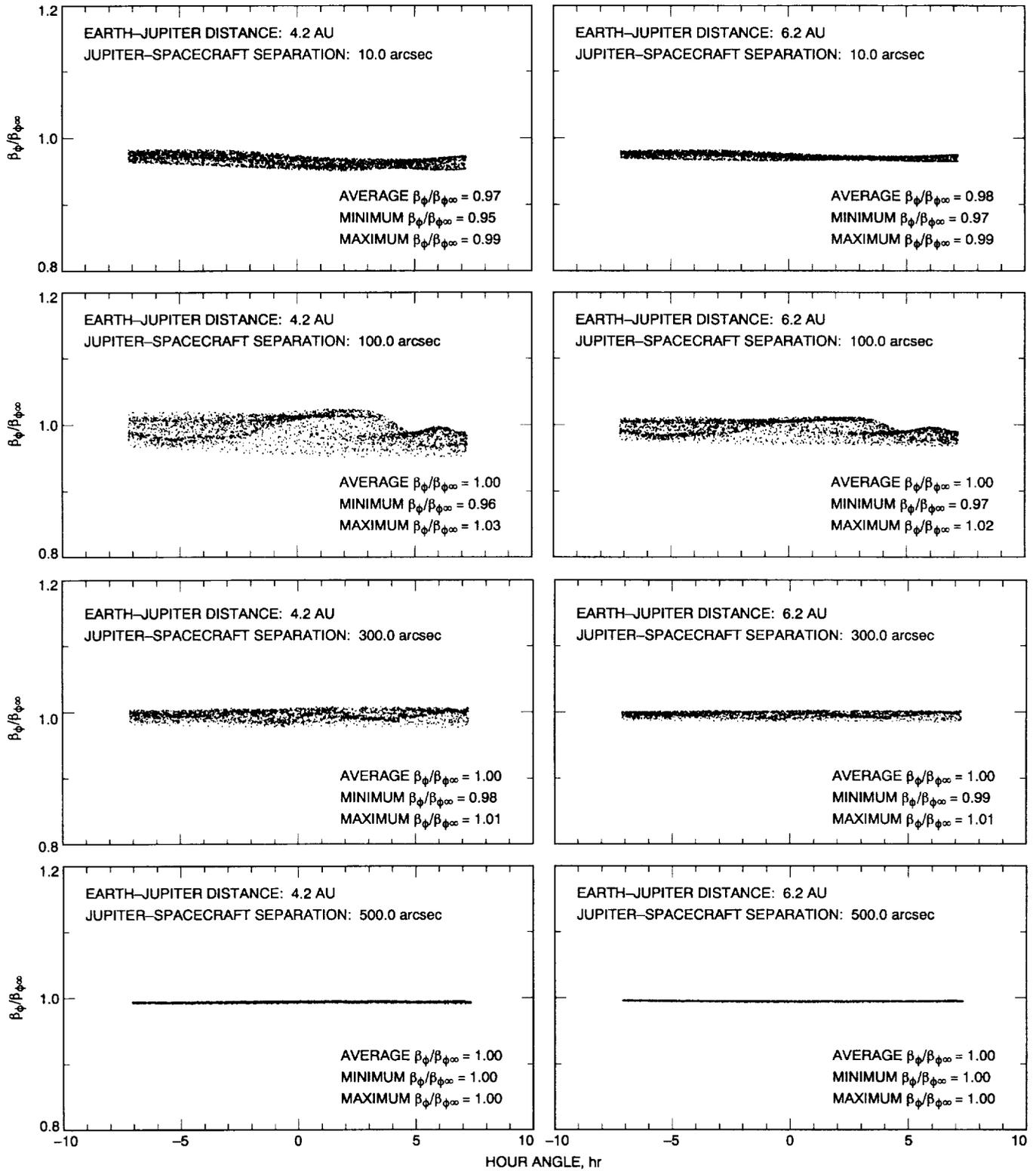Fig. 2. A simplified block diagram of an array signal path.

Fig. 3. The ratio of $\beta_\phi/\beta_{\phi\infty}$ for an array of antennas at the DSN Canberra complex observing Jupiter and a spacecraft at S-band, for a variety of array and source geometries. The declination of Jupiter = -21.0 deg and the array consists of DSS 43, DSS 42, DSS 45, and DSS 34.
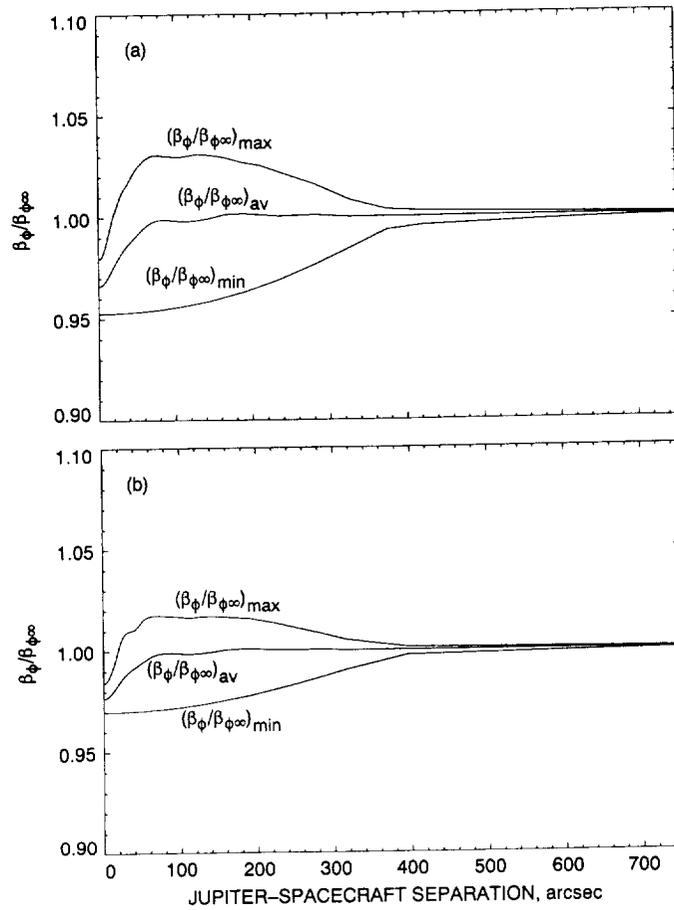
Fig. 4. The average, minimum, and maximum values of $\beta_\phi / \beta_{\phi\infty}$ obtained as source orientation is varied, plotted as a function of the separation between the spacecraft and the center of Jupiter, with Jupiter declination = -21.0 deg: (a) Earth–Jupiter distance = 4.2 AU and (b) Earth–Jupiter distance = 6.2 AU.

Appendix A

Basic Expressions

I. Incoming Signals

The voltage (as a function of time t and sky frequency ν_{sky}) induced in a single polarization channel at $\mathbf{r}_i$, the focal point of the ith antenna, by a distant[8] source (e.g., a planet or spacecraft) can be written

$$V_i(\nu_{sky}, t) = e^{i\phi_i} \sqrt{k_B G_i} \iint d\hat{s}\, f_i(\hat{s} - \hat{s}_0) \mathcal{I}(\nu_{sky}, t, \hat{s}) e^{i(2\pi\nu_{sky}[t - (\hat{s}\cdot\mathbf{r}_i/c)] + \theta(\nu_{sky}, \hat{s}))} \tag{A-1}$$

In this expression, k_B represents Boltzmann's constant and c is the speed of light; G_i is the on-axis antenna gain, f_i is the magnitude of the antenna's field pattern, $\hat{s}$ is a unit vector in the direction of the source, $\mathcal{I}(\nu_{sky}, t, \hat{s})$ is the amplitude of the electric field due to the source, $\theta(\nu_{sky}, \hat{s})$ is a phase term (which for most astronomical sources can be assumed to be uncorrelated over ν_{sky} and $\hat{s}$), and ϕ_i is an antenna-based phase shift (including atmospheric effects).

The voltage induced by system noise can be written

$$V_i^N(\nu_{sky}, t) = \sqrt{k_B T_i}\, e^{i\left(2\pi\nu_{sky}t + \theta_i^N(\nu_{sky}, t)\right)} \tag{A-2}$$

where T_i is the noise temperature and $\theta_i^N(\nu_{sky}, t)$ is a random phase that is uncorrelated over time and frequency intervals satisfying $\Delta\nu_{sky}\Delta t \gtrsim 1$. The total RF voltage can be written as the sum of terms due to the spacecraft, planet, and system noise:

$$V_i(\nu_{sky}, t) = V_i^{s/c}(\nu_{sky}, t) + V_i^P(\nu_{sky}, t) + V_i^N(\nu_{sky}, t) \tag{A-3}$$

When the RF signal is mixed to baseband, it is phase shifted by $2\pi\nu_{lo}\tau_i^m$; this stops the fringes, allowing time averaging over a longer interval. An additional phase shift $-\phi_i^m$ can be inserted to (attempt to) compensate for the antenna-based phase shifts ϕ_i. Without this additional phase shift, the baseband voltage can be written

$$v_i(\nu, t) = e^{i2\pi\nu_{lo}\tau_i^m} e^{-i2\pi\nu_{lo}t} V_i(\nu_{sky}, t)$$

$$= e^{i2\pi\nu_{lo}[\tau_i^m - t]} \left[V_i^{s/c}(\nu_{sky}, t) + V_i^P(\nu_{sky}, t) + V_i^N(\nu_{sky}, t)\right]$$

$$= e^{i(2\pi\nu_{lo}[\tau_i^m - t] + \phi_i)} \sqrt{k_B G_i} \iint d\hat{s}\, f_i(\hat{s} - \hat{s}_0) e^{i2\pi\nu_{sky}[t - (\hat{s}\cdot\mathbf{r}_i/c)]} \left[\mathcal{I}_{s/c}(\nu_{sky}, t, \hat{s}) e^{i\theta^{s/c}(\nu_{sky}, \hat{s})}\right.$$

$$\left. + \mathcal{I}_P(\nu_{sky}, t, \hat{s}) e^{i\theta^P(\nu_{sky}, \hat{s})}\right] + e^{i2\pi\nu_{lo}[\tau_i^m - t]} \sqrt{k_B T_i}\, e^{i\left(2\pi\nu_{sky}t + \theta_i^N(\nu_{sky}, t)\right)}$$

$$= e^{i\phi_i} \sqrt{k_B G_i} \iint d\hat{s}\, f_i(\hat{s} - \hat{s}_0) e^{i2\pi(\nu[t - (\hat{s}\cdot\mathbf{r}_i/c)] + \nu_{lo}[\tau_i^m - (\hat{s}\cdot\mathbf{r}_i/c)])} \left[\mathcal{I}_{s/c}(\nu_{sky}, t, \hat{s}) e^{i\theta^{s/c}(\nu_{sky}, \hat{s})}\right.$$

$$\left. + \mathcal{I}_P(\nu_{sky}, t, \hat{s}) e^{i\theta^P(\nu_{sky}, \hat{s})}\right] + \sqrt{k_B T_i}\, e^{i\left(2\pi[\nu t + \nu_{lo}\tau_i^m] + \theta_i^N(\nu_{sky}, t)\right)} \tag{A-4}$$

---

[8] Here, "distant" means a source sufficiently far away that, over the extent of the array, a plane wave approximation is valid.

where $\nu = \nu_{sky} - \nu_{lo}$ is the baseband frequency. Like the RF voltage, the baseband voltage can be written as the sum of terms due to the spacecraft, planet, and system noise:

$$v_i(\nu, t) = v_i^{s/c}(\nu, t) + v_i^P(\nu, t) + v_i^N(\nu, t) \tag{A-5}$$

If the additional phase shift is inserted, the baseband signal has the form $e^{-i\phi_i^m} v_i(\nu, t)$.

II. Single-Dish Power

For the ith antenna, the single-dish power can be written

$$P_i = \left\langle \int_0^{\Delta\nu} d\nu \, |v_i(\nu, t)|^2 \right\rangle_T$$

$$= \left\langle \int_0^{\Delta\nu} d\nu \, |v_i^{s/c}(\nu, t) + v_i^P(\nu, t) + v_i^N(\nu, t)|^2 \right\rangle_T$$

$$= \left\langle \int_0^{\Delta\nu} d\nu \left[v_i^{s/c}(\nu, t)v_i^{s/c\,*}(\nu, t) + v_i^P(\nu, t)v_i^{s/c\,*}(\nu, t) + v_i^N(\nu, t)v_i^{s/c\,*}(\nu, t) \right. \right.$$

$$+ v_i^{s/c}(\nu, t)v_i^{P\,*}(\nu, t) + v_i^P(\nu, t)v_i^{P\,*}(\nu, t) + v_i^N(\nu, t)v_i^{P\,*}(\nu, t)$$

$$\left. \left. + v_i^{s/c}(\nu, t)v_i^{N\,*}(\nu, t) + v_i^P(\nu, t)v_i^{N\,*}(\nu, t) + v_i^N(\nu, t)v_i^{N\,*}(\nu, t) \right] \right\rangle_T \tag{A-6}$$

where the angle brackets denote a time average and T is the interval over which the time average is taken. Looking at each term separately and considering the planet term first,

$$v_i^P(\nu, t)v_i^{P\,*}(\nu, t) = e^{i\phi_i}\sqrt{k_B G_i} \iint d\hat{s} \, f_i(\hat{s} - \hat{s}_0)e^{i2\pi(\nu[t-(\hat{s}\cdot r_i/c)]+\nu_{lo}[\tau_i^m -(\hat{s}\cdot r_i/c)])} \mathcal{I}_P(\nu + \nu_{lo}, t, \hat{s})e^{i\theta^P(\nu+\nu_{lo}, \hat{s})}$$

$$\times \, e^{-i\phi_i}\sqrt{k_B G_i} \iint d\hat{s}' \, f_i(\hat{s}' - \hat{s}_0)e^{-i2\pi(\nu[t-(\hat{s}'\cdot r_i/c)]+\nu_{lo}[\tau_i^m -(\hat{s}'\cdot r_i/c)])} \mathcal{I}_P(\nu + \nu_{lo}, t, \hat{s}')e^{-i\theta^P(\nu+\nu_{lo}, \hat{s}')}$$

$$= k_B G_i \iint d\hat{s} \, f_i(\hat{s} - \hat{s}_0)\mathcal{I}_P(\nu + \nu_{lo}, t, \hat{s}) \iint d\hat{s}' \left\{ e^{-i(2\pi(\nu[\hat{s}-\hat{s}']\cdot r_i +\nu_{lo}[\hat{s}-\hat{s}']\cdot r_i)/c)} \right.$$

$$\left. \times \, e^{i[\theta^P(\nu+\nu_{lo}, \hat{s})-\theta^P(\nu+\nu_{lo}, \hat{s}')]} f_i(\hat{s}' - \hat{s}_0)\mathcal{I}_P(\nu + \nu_{lo}, t, \hat{s}') \right\}$$

$$= k_B G_i \iint d\hat{s} \, f_i^2(\hat{s} - \hat{s}_0)\mathcal{I}_P^2(\nu + \nu_{lo}, t, \hat{s})$$

$$= k_B G_i \iint d\hat{s} \, f_i^2(\hat{s} - \hat{s}_0)I_P(\nu + \nu_{lo}, t, \hat{s}) \tag{A-7}$$

where the integral over $\hat{s}'$ is nonzero only when $\hat{s}' = \hat{s}$ because the radiation from the planet is spatially incoherent, and where the substitution $\mathcal{I}_P^2(\nu + \nu_{lo}, t, \hat{s}) = I_P(\nu + \nu_{lo}, t, \hat{s})$ was made; I_P is the brightness distribution (flux per unit solid angle) of the planet. Similarly

$$v_i^{s/c}(\nu,t)v_i^{s/c*}(\nu,t) = k_B G_i \iint d\hat{s}\ f_i^2(\hat{s} - \hat{s}_0)I_{s/c}(\nu + \nu_{lo}, t, \hat{s}) \tag{A-8}$$

with $I_{s/c}$ being the brightness distribution of the spacecraft (usually assumed to be pointlike), and

$$v_i^N(\nu,t)v_i^{N,*}(\nu,t) = k_B T_i \tag{A-9}$$

Compared to these terms, the cross terms are all small, as can be seen by considering

$$v_i^{s/c}(\nu,t)v_i^{P*}(\nu,t) = k_B G_i \iint_{s/c} d\hat{s}\ f_i(\hat{s} - \hat{s}_0)\mathcal{I}_{s/c}(\nu + \nu_{lo}, t, \hat{s}) \iint_P d\hat{s}'\ \left\{ e^{-i(2\pi/c)(\nu[\hat{s}-\hat{s}']\cdot\mathbf{r}_i + \nu_{lo}[\hat{s}-\hat{s}']\cdot\mathbf{r}_i)} \right.$$

$$\left. \times\ e^{i[\theta^{s/c}(\nu+\nu_{lo},\hat{s})-\theta^P(\nu+\nu_{lo},\hat{s}')]} f_i(\hat{s}' - \hat{s}_0)\mathcal{I}_P(\nu + \nu_{lo}, t, \hat{s}') \right\}$$

$$\approx 0 \tag{A-10}$$

where the integral over $\hat{s}'$ is small because $\theta^{s/c}$ and θ^P are uncorrelated [unlike in Eqs. (A-7) and (A-8), this integral is, on average, zero, even when $\hat{s}' = \hat{s}$].

One can therefore write

$$P_i = \left\langle \int_0^{\Delta\nu} d\nu\ |v_i(\nu,t)|^2 \right\rangle_T$$

$$= \left\langle \int_0^{\Delta\nu} d\nu\ |v_i^{s/c}(\nu,t)|^2 + |v_i^P(\nu,t)|^2 + |v_i^N(\nu,t)|^2 \right\rangle_T$$

$$= P_i^{s/c} + P_i^P + P_i^N \tag{A-11}$$

It is assumed that the spacecraft is a point source located at $\hat{s}_{s/c}$, transmitting a narrowband, polarized signal at a sky frequency $\nu_{sky}^{s/c}$ with a total power $\mathcal{P}_{s/c}$. The brightness distribution seen by a receiver matched to the signal's polarization[9] is

$$I_{s/c}(\nu_{sky}, t, \hat{s}) = 2\mathcal{P}_{s/c}\delta\left(\nu_{sky} - \nu_{sky}^{s/c}\right)\delta(\hat{s} - \hat{s}_{s/c}) \tag{A-12}$$

(with δ representing a Dirac delta function), so

---

[9] The factor of 2 in Eq. (A-12) arises from the assumption of matched polarizations.

$$P_i^{s/c} = 2k_B f_i^2(\hat{s}_{s/c} - \hat{s}_0)G_i \mathcal{P}_{s/c} \approx 2k_B G_i \mathcal{P}_{s/c} \tag{A-13}$$

where it is assumed that $f_i^2(\hat{s}_{s/c} - \hat{s}_0) \approx 1$ (i.e., the spacecraft is close to center of the array's field of view).

It is assumed that the planet is an extended, unpolarized, broadband source of total flux at the frequencies of interest of S_P, which is constant in time and varies only slowly with frequency (i.e., it can be considered constant across the observing bandwidth $\Delta\nu$), so $I_P(\nu_{sky}, t, \hat{s}) = I_P(\hat{s})$ and

$$P_i^P = k_B G_i \Delta\nu \iint_P d\hat{s}\, f_{i_P}^2(\hat{s} - \hat{s}_0) I_P(\hat{s}) = k_B \bar{f}_{i_P}^2 G_i \Delta\nu S_P \tag{A-14}$$

where $\bar{f}_{i_P}^2$ is a weighted average of $f_{i_P}^2$ over the planet.

Finally, from Eq. (A-9)

$$P_i^N = k_B T_i \Delta\nu \tag{A-15}$$

III. Cross-Correlation

The cross-correlation of the voltages from the ith and kth antennas is given by

$$\rho_{ik} = \left\langle \int_0^{\Delta\nu} d\nu\, e^{i(\phi_k^m - \phi_i^m)} v_i(\nu, t + \tau_i^m) v_k^*(\nu, t + \tau_k^m) \right\rangle_T \tag{A-16}$$

By using the general form of the baseband signal [Eq. (A-4)] and because the signal is spatially incoherent, this becomes

$$\rho_{ik} = \left\langle \int_0^{\Delta\nu} d\nu\, e^{i(\phi_k^m - \phi_i^m)} \left[v_i^{s/c}(\nu, t + \tau_i^m) + v_i^P(\nu, t + \tau_i^m) + v_i^N(\nu, t + \tau_i^m) \right] \right.$$

$$\left. \times \left[v_k^{*s/c}(\nu, t + \tau_k^m) + v_k^{*P}(\nu, t + \tau_k^m) + v_k^{*N}(\nu, t + \tau_k^m) \right] \right\rangle_T$$

$$= \left\langle \int_0^{\Delta\nu} d\nu\, e^{i(\phi_k^m - \phi_i^m)} \left[v_i^{s/c}(\nu, t + \tau_i^m) v_k^{*s/c}(\nu, t + \tau_k^m) + v_i^P(\nu, t + \tau_i^m) v_k^{*s/c}(\nu, t + \tau_k^m) \right. \right.$$

$$+ v_i^N(\nu, t + \tau_i^m) v_k^{*s/c}(\nu, t + \tau_k^m) + v_i^{s/c}(\nu, t + \tau_i^m) v_k^{*P}(\nu, t + \tau_k^m)$$

$$+ v_i^P(\nu, t + \tau_i^m) v_k^{*P}(\nu, t + \tau_k^m) + v_i^N(\nu, t + \tau_i^m) v_k^{*P}(\nu, t + \tau_k^m)$$

$$+ v_i^{s/c}(\nu, t + \tau_i^m) v_k^{*N}(\nu, t + \tau_k^m) + v_i^P(\nu, t + \tau_i^m) v_k^{*N}(\nu, t + \tau_k^m)$$

$$\left. \left. + v_i^N(\nu, t + \tau_i^m) v_k^{*N}(\nu, t + \tau_k^m) \right] \right\rangle_T \tag{A-17}$$

This can be written as

$$\rho_{ik} = \rho_{ik}^{s/c} + \rho_{ik}^{P} + \rho_{ik}^{N}$$

(A-18)

where

$$\rho_{ik}^{s/c} = \left\langle \int_0^{\Delta\nu} d\nu\, e^{i(\phi_k^m - \phi_i^m)} v_i^{s/c}(\nu, t + \tau_i^m) v_k^{*s/c}(\nu, t + \tau_k^m) \right\rangle_{\mathcal{T}}$$

(A-19)

$$\rho_{ik}^{P} = \left\langle \int_0^{\Delta\nu} d\nu\, e^{i(\phi_k^m - \phi_i^m)} v_i^{P}(\nu, t + \tau_i^m) v_k^{*P}(\nu, t + \tau_k^m) \right\rangle_{\mathcal{T}}$$

(A-20)

$$\rho_{ik}^{N} = \left\langle \int_0^{\Delta\nu} d\nu\, e^{i(\phi_k^m - \phi_i^m)} \left[v_i^{N}(\nu, t + \tau_i^m) v_k^{*N}(\nu, t + \tau_k^m) + v_i^{P}(\nu, t + \tau_i^m) v_k^{*s/c}(\nu, t + \tau_k^m) \right. \right.$$

$$+ v_i^{N}(\nu, t + \tau_i^m) v_k^{*s/c}(\nu, t + \tau_k^m) + v_i^{s/c}(\nu, t + \tau_i^m) v_k^{*P}(\nu, t + \tau_k^m)$$

$$+ v_i^{N}(\nu, t + \tau_i^m) v_k^{*P}(\nu, t + \tau_k^m) + v_i^{s/c}(\nu, t + \tau_i^m) v_k^{*N}(\nu, t + \tau_k^m)$$

$$\left. \left. + v_i^{P}(\nu, t + \tau_i^m) v_k^{*N}(\nu, t + \tau_k^m) \right] \right\rangle_{\mathcal{T}}$$

(A-21)

These expressions are similar in structure to the expression for single-dish power [Eq. (A-6)]. Looking at ρ_{ik}^{P}, one finds

$$v_i^{P}(\nu, t + \tau_i^m) v_k^{*P}(\nu, t + \tau_k^m) = e^{i(\phi_i - \phi_k)} k_B \sqrt{G_i G_k}\, e^{i2\pi[\nu + \nu_{lo}][\tau_i^m - \tau_k^m]} \left[\iint d\hat{s} \left\{ e^{-i(2\pi[\nu + \nu_{lo}]\hat{s}\cdot\mathbf{r}_i/c)} f_i(\hat{s} - \hat{s}_0) \mathcal{I}_P(\hat{s}) \right.\right.$$

$$\times \iint d\hat{s}'\, f_k(\hat{s}' - \hat{s}_0) \mathcal{I}_P(\hat{s}') e^{i\left(2\pi[\nu + \nu_{lo}]\hat{s}'\cdot\mathbf{r}_k/c\right)} e^{i\left(\theta^P(\nu + \nu_{lo}, \hat{s}) - \theta^P(\nu + \nu_{lo}, \hat{s}')\right)} \left. \left. \right\} \right]$$

$$= e^{i(\phi_i - \phi_k)} k_B \sqrt{G_i G_k}\, e^{i(2\pi[\nu + \nu_{lo}][\hat{s}_0\cdot\mathbf{r}_i - \hat{s}_0\cdot\mathbf{r}_k]/c)}$$

$$\times \iint d\hat{s}\, e^{i(2\pi[\nu + \nu_{lo}]\hat{s}\cdot[\mathbf{r}_k - \mathbf{r}_i]/c)} f_i(\hat{s} - \hat{s}_0) f_k(\hat{s} - \hat{s}_0) I_P(\hat{s})$$

$$= e^{i(\phi_i - \phi_k)} k_B \sqrt{G_i G_k} \iint d\hat{s}\, e^{i(2\pi[\nu + \nu_{lo}][\hat{s} - \hat{s}_0]\cdot[\mathbf{r}_k - \mathbf{r}_i]/c)} f_i(\hat{s} - \hat{s}_0) f_k(\hat{s} - \hat{s}_0) I_P(\hat{s})$$

$$= e^{i(\phi_i - \phi_k)} k_B \sqrt{G_i G_k} \iint d\hat{s}\, e^{i(2\pi[\nu + \nu_{lo}][\hat{s} - \hat{s}_0]\cdot\mathbf{B}_{ik}/c)} f_i(\hat{s} - \hat{s}_0) f_k(\hat{s} - \hat{s}_0) I_P(\hat{s})$$

(A-22)

where the substitutions $\tau_i^m = \hat{s}_0 \cdot r_i / c$, $\tau_k^m = \hat{s}_0 \cdot r_k / c$ and $B_{ik} = r_k - r_i$ have been made.

Similarly

$$v_i^{s/c}(\nu, t + \tau_i^m) v_k^{*s/c}(\nu, t + \tau_k^m) = e^{i(\phi_i - \phi_k)} k_B \sqrt{G_i G_k}$$

$$\times \iint d\hat{s} \, e^{i(2\pi[\nu + \nu_{lo}][\hat{s} - \hat{s}_0] \cdot B_{ik}/c)} f_i(\hat{s} - \hat{s}_0) f_k(\hat{s} - \hat{s}_0) I_{s/c}(\hat{s}) \qquad \text{(A-23)}$$

In considering the effects of noise, it is assumed[10] that Eq. (A-21) can be approximated as

$$\rho_{ik}^N \approx \left\langle \int_0^{\Delta\nu} d\nu \, e^{i(\phi_k^m - \phi_i^m)} v_i^N(\nu, t + \tau_i^m) v_k^{*N}(\nu, t + \tau_k^m) \right\rangle_T$$

$$\approx k_B \sqrt{T_i T_k} \left\langle \int_0^{\Delta\nu} d\nu \, e^{i(\phi_k^m - \phi_i^m)} e^{i(2\pi\nu[t + \tau_i^m] + 2\pi\nu_{lo}\tau_i^m + \theta_i^N(\nu_{sky}, t + \tau_i^m))} e^{-i(2\pi\nu[t + \tau_k^m] + 2\pi\nu_{lo}\tau_k^m + \theta_k^N(\nu_{sky}, t + \tau_k^m))} \right\rangle_T$$

$$\approx k_B \sqrt{T_i T_k} \left\langle \int_0^{\Delta\nu} d\nu \, e^{i(2\pi\nu[\tau_i^m - \tau_k^m] + 2\pi\nu_{lo}[\tau_i^m - \tau_k^m] + \phi_k^m - \phi_i^m + \theta_i^N(\nu_{sky}, t + \tau_i^m) - \theta_k^N(\nu_{sky}, t + \tau_k^m))} \right\rangle_T$$

$$\approx k_B \sqrt{T_i T_k} \frac{\sqrt{\Delta\nu T}}{T} e^{i\theta_{ik}^N}$$

$$\approx k_B \sqrt{T_i T_k} \sqrt{\frac{\Delta\nu}{T}} e^{i\theta_{ik}^N} \qquad \text{(A-24)}$$

where θ_{ik}^N is a phase randomly distributed between 0 and 2π, and where use has been made of the fact that $\theta_i^N(\nu_{sky}, t)$ is uncorrelated between antennas and over time and frequency intervals where $\Delta\nu T > 1$. Because the phases of ρ_{ik}^N are random, the double sum in Eq. (10) will be small. However, as discussed in Appendix C, noise terms become important when the process of phasing the array is considered.

Using Eq. (A-12) to substitute for $I_{s/c}$,

$$\rho_{ik}^{s/c} = 2P_{s/c} \left\langle \int_0^{\Delta\nu} d\nu \, \delta(\nu - [\nu_{sky}^{s/c} - \nu_{lo}]) e^{i(\phi_k^m - \phi_i^m)} e^{i(\phi_i - \phi_k)} k_B \sqrt{G_i G_k} \right.$$

$$\left. \times \iint d\hat{s} \, e^{i(2\pi[\nu + \nu_{lo}][\hat{s} - \hat{s}_0] \cdot B_{ik}]/c)} f_i(\hat{s} - \hat{s}_0) f_k(\hat{s} - \hat{s}_0) \delta(\hat{s} - \hat{s}_{s/c}) \right\rangle_T$$

$$= 2P_{s/c} k_B \sqrt{G_i G_k} e^{i(\delta\phi_i - \delta\phi_k)} e^{i(2\pi\nu_{sky}^{s/c}[\hat{s}_{s/c} - \hat{s}_0] \cdot B_{ik}/c)} f_i(\hat{s}_{s/c} - \hat{s}_0) f_k(\hat{s}_{s/c} - \hat{s}_0) \qquad \text{(A-25)}$$

---

[10] This assumption is not valid if the planet or the spacecraft contributes significantly to the system temperature; in that case, the cross terms in Eq. (A-21) will be non-negligible. However, they can be treated in a manner similar to the $v^N v^{*N}$ term.

Note that $\hat{s}_{s/c} - \hat{s}_0$ must be small enough that the quantity $\nu_{sky}^{s/c}[\hat{s}_{s/c} - \hat{s}_0]\cdot \mathbf{B}_{ik}/c$ does not change significantly over the interval of the time averaging.

Similarly,

$$\rho_{ik}^P = k_B \sqrt{G_i G_k}\, e^{i(\delta\phi_i - \delta\phi_k)} \left\langle \iint d\hat{s}\, f_i(\hat{s} - \hat{s}_0) f_k(\hat{s} - \hat{s}_0) I_P(\hat{s}) \int_0^{\Delta\nu} d\nu\, e^{i(2\pi[\nu + \nu_{lo}][\hat{s} - \hat{s}_0]\cdot \mathbf{B}_{ik}/c)} \right\rangle_T \qquad (A\text{-}26)$$

At this point, it is useful to define the quantity

$$\mathcal{F}_{ik}^P \equiv \frac{1}{\Delta\nu S_P} \iint d\hat{s}\, e^{i(2\pi\nu_{lo}\mathbf{B}_{ik}\cdot(\hat{s} - \hat{s}_0)/c)} f_i(\hat{s} - \hat{s}_0) f_k(\hat{s} - \hat{s}_0) I_P(\hat{s}) \int_0^{\Delta\nu} d\nu\, e^{i(2\pi\nu\mathbf{B}_{ik}\cdot(\hat{s} - \hat{s}_0)/c)} \qquad (A\text{-}27)$$

so that

$$\rho_{ik}^P = \Delta\nu\, k_B S_P \sqrt{G_i G_k}\, e^{i(\delta\phi_i - \delta\phi_k)} \mathcal{F}_{ik}^P \qquad (A\text{-}28)$$

$\mathcal{F}_{ik}^P$ is a dimensionless complex quantity that depends only on the array geometry and the source structure and whose magnitude is always less than or equal to unity ($|\mathcal{F}_{ik}^P| \to 1$ in the short baseline limit, and $|\mathcal{F}_{ik}^P| \to 0$ in the long baseline limit).

It has been implicitly assumed that the bandpass is rectangular, in which case the integral over ν can be simplified:

$$\int_0^{\Delta\nu} d\nu\, e^{i(2\pi\nu\mathbf{B}_{ik}\cdot(\hat{s} - \hat{s}_0)/c)} = e^{i(\pi\Delta\nu\mathbf{B}_{ik}\cdot[\hat{s} - \hat{s}_0]/c)}\mathrm{sinc}\left(\frac{\Delta\nu}{c}\mathbf{B}_{ik}\cdot[\hat{s} - \hat{s}_0]\right) \qquad (A\text{-}29)$$

where $\mathrm{sinc}(x) = \sin(\pi x)/\pi x$. This term, often referred to as the delay beam, introduces a phase shift and lowers the correlation amplitude for $\hat{s} \neq \hat{s}_0$; both these effects are more pronounced for larger bandwidths $\Delta\nu$.

One can therefore write

$$\mathcal{F}_{ik}^P = \frac{1}{\Delta\nu S_P} \iint d\hat{s}\, e^{i(2\pi\nu_{sky}^c \mathbf{B}_{ik}\cdot(\hat{s} - \hat{s}_0)/c)} f_i(\hat{s} - \hat{s}_0) f_k(\hat{s} - \hat{s}_0) I_P(\hat{s})\, \mathrm{sinc}\left(\frac{\Delta\nu}{c}\mathbf{B}_{ik}\cdot[\hat{s} - \hat{s}_0]\right) \qquad (A\text{-}30)$$

where $\nu_{sky}^c = \nu_{lo} + \Delta\nu/2$.

If the quantities f_i, f_k and $\mathrm{sinc}(\Delta\nu\mathbf{B}_{ik}\cdot[\hat{s} - \hat{s}_0]/c)$ do not vary greatly over the extent of the planet, one can make the further simplification

$$\mathcal{F}_{ik}^P = \frac{1}{\Delta\nu S_P} \bar{f}_{i_P} \bar{f}_{k_P} \bar{f}_{\Delta\nu\, ik} \iint d\hat{s}\, e^{i(2\pi\nu_{sky}^c \mathbf{B}_{ik}\cdot(\hat{s} - \hat{s}_0)/c)} I_P(\hat{s}) \qquad (A\text{-}31)$$

where $\bar{f}_{i_P}, \bar{f}_{k_P}, \bar{f}_{\Delta\nu\, ik}$ are suitably weighted averages of f_i, f_k and $\mathrm{sinc}(\Delta\nu\mathbf{B}_{ik}\cdot[\hat{s} - \hat{s}_0]/c)$, respectively.

Appendix B

Jupiter Model

At centimeter wavelengths, Jupiter is not a simple thermal disk; there is significant synchrotron emission from the radiation belts and the resulting flux distribution is quite complicated [6,7]. For the purposes of this article, Jupiter can be modelled as the sum of three components: two circular (2-dimensional) Gaussian components (representing the radiation belts) and a uniform central disk. This is a simple model to work with because Eq. (A-27) can be integrated analytically for each of these components.

If the brightness distribution of a source is radially symmetric about the point $\hat{s}_C$, small compared to the delay beam, and small compared to the primary beam of any antenna, Eq. (A-27) can be written

$$\mathcal{F}_{ik} = \frac{2\bar{f}_i\bar{f}_k}{S}\bar{f}_{\Delta\nu_{ik}}e^{i(2\pi\nu^c_{sky}\mathbf{B}_{ik}\cdot[\hat{s}_C-\hat{s}_0]/c)}\int_0^\infty r\,dr\,I(r)J_0\left(\frac{2\pi\nu^c_{sky}B_{ik}r}{c}\right) \tag{B-1}$$

where $r = |\hat{s} - \hat{s}_C|$; $\bar{f}_{\Delta\nu_{ik}}$ is the value of the delay beam at the source; $\bar{f}_i$, $\bar{f}_k$ are the average values of the antenna; field pattern at the source; for the ith and kth antenna; S is the total flux of the source; $I(r)$ is the source's radially symmetric brightness distribution; and J_0 is a zeroth-order Bessel function.

For a uniform disk of angular radius R_D centered at $\hat{s}_C$,

$$I(r) = \frac{S}{\pi R_D^2} \qquad r \leq R_D$$

$$= 0 \qquad r > R_D \tag{B-2}$$

$$\mathcal{F}^D_{ik} = \bar{f}_i\bar{f}_k\bar{f}_{\Delta\nu_{ik}}e^{i(2\pi\nu^c_{sky}/c)\mathbf{B}_{ik}\cdot(\hat{s}_D-\hat{s}_0)}\frac{cJ_1(2\pi\nu^c_{sky}B_{ik}R_D/c)}{\pi\nu^c_{sky}B_{ik}R_D} \tag{B-3}$$

For a circular Gaussian of total flux S and characteristic size (1/e radius) R_G, centered at $\hat{s}_C$,

$$I(r) = \frac{S}{\pi R_G^2}e^{-r^2/R_G^2} \tag{B-4}$$

and Eq. (B-1) becomes

$$\mathcal{F}^G_{ik} = \bar{f}_i\bar{f}_k\bar{f}_{\Delta\nu_{ik}}e^{i(2\pi\nu^c_{sky}\mathbf{B}_{ik}\cdot[\hat{s}_C-\hat{s}_0]/c)}\frac{e^{-(\pi\nu^c_{sky}B_{ik}R_G/c)^2}}{\pi} \tag{B-5}$$

Jupiter's brightness distribution is modelled as the sum of a uniform central disk of radius R_J, centered at $\hat{s}_J$, and two circular Gaussians of characteristic size R_B, representing the radiation belts, which are offset from the center of the disk by $\pm\Delta s_B$. The flux of the central disk is written as $F_D S_J$, where S_J is the total flux of Jupiter and F_D is the fraction of that flux in the disk; the integrated flux of each wing component can be written as $(1 - F_D)S_J/2$. Using this model with Eqs. (B-3) and (B-5),

$$\mathcal{F}_{ik}^J = \bar{f}_i^J \bar{f}_k^J \bar{f}_{\Delta\nu_{ik}}^J e^{i(2\pi\nu_{sky}^c \mathbf{B}_{ik}\cdot[\hat{\mathbf{s}}_J - \hat{\mathbf{s}}_0]/c)}\left[F_D \frac{cJ_1(2\pi\nu_{sky}^c B_{ik}R_J/c)}{\pi\nu_{sky}^c B_{ik}R_J}\right.$$

$$\left. + (1 - F_D)\frac{e^{-(\pi\nu_{sky}^c B_{ik}R_B/c)^2}}{\pi}\cos\left(\frac{2\pi\nu_{sky}^c}{c}\mathbf{B}_{ik}\cdot\Delta\mathbf{s}_B\right)\right] \tag{B-6}$$

If the above expression and Eq. (C-1), the condition that the array is properly phased on the spacecraft, are substituted into Eq. (A-28), one gets, for the cross-correlation due to Jupiter in a phased array,

$$\rho_{ik}^J = \Delta\nu k_B S_J \sqrt{G_i G_k}\, \bar{f}_i^J \bar{f}_k^J \bar{f}_{\Delta\nu_{ik}}^J e^{i(2\pi\mathbf{B}_{ik}\cdot(\nu_{sky}^c[\hat{\mathbf{s}}_J-\hat{\mathbf{s}}_0]-\nu_{sky}^{s/c}[\hat{\mathbf{s}}_{s/c}-\hat{\mathbf{s}}_0])/c)}$$

$$\times\left[F_D \frac{cJ_1(2\pi\nu_{sky}^c B_{ik}R_J/c)}{\pi\nu_{sky}^c B_{ik}R_J} + (1 - F_D)\frac{e^{-(\pi\nu_{sky}^c B_{ik}R_B/c)^2}}{\pi}\cos\left(\frac{2\pi\nu_{sky}^c}{c}\mathbf{B}_{ik}\cdot\Delta\mathbf{s}_B\right)\right] \tag{B-7}$$

In the case where $\hat{\mathbf{s}}_{s/c} = \hat{\mathbf{s}}_0$ and/or $\nu_{sky}^{s/c} = \nu_{sky}^c$, this simplifies to

$$\rho_{ik}^J = \Delta\nu k_B S_J \sqrt{G_i G_k}\, \bar{f}_i^J \bar{f}_k^J \bar{f}_{\Delta\nu_{ik}}^J e^{i(2\pi\nu_{sky}^c \mathbf{B}_{ik}\cdot[\hat{\mathbf{s}}_J-\hat{\mathbf{s}}_{s/c}]/c)}$$

$$\times\left[F_D \frac{cJ_1(2\pi\nu_{sky}^c B_{ik}R_J/c)}{\pi\nu_{sky}^c B_{ik}R_J} + (1 - F_D)\frac{e^{-(\pi\nu_{sky}^c B_{ik}R_B/c)^2}}{\pi}\cos\left(\frac{2\pi\nu_{sky}^c}{c}\mathbf{B}_{ik}\cdot\Delta\mathbf{s}_B\right)\right] \tag{B-8}$$

Both the total flux S_J and the flux distribution are functions of frequency and Earth–Jupiter distance. From the data given in [5], the model at S-band (2.3 GHz) used in this article is

$$S_J = 6.3\left(\frac{4.04\,\mathrm{AU}}{d}\right)^2 \mathrm{Jy}$$

$$F_D = 0.3$$

$$R_J = 24.3\,\frac{4.04\,\mathrm{AU}}{d}\,\mathrm{arcsec}$$

$$|\Delta\mathbf{s}_B| \approx 2R_J$$

$$R_B \approx 1.3R_J \tag{B-9}$$

At conjunction, $d = 6.2$ AU, $S_J = 2.7$ Jy, and $R_J = 15.8$ arcsec; at opposition, $d = 4.2$ AU, $S_J = 5.8$ Jy, and $R_J = 23.4$ arcsec.

Figure B-1(a) shows a map of Jupiter from [6] at 2.9 GHz (10.4 cm), while Fig. B-1(b) shows a higher resolution map from [7] at 1.4 GHz. Note that in Fig. B-1(b), the disk has not been removed. Figure (B-2) shows the model of Jupiter used in this article in the same format as Fig. B-1(a).
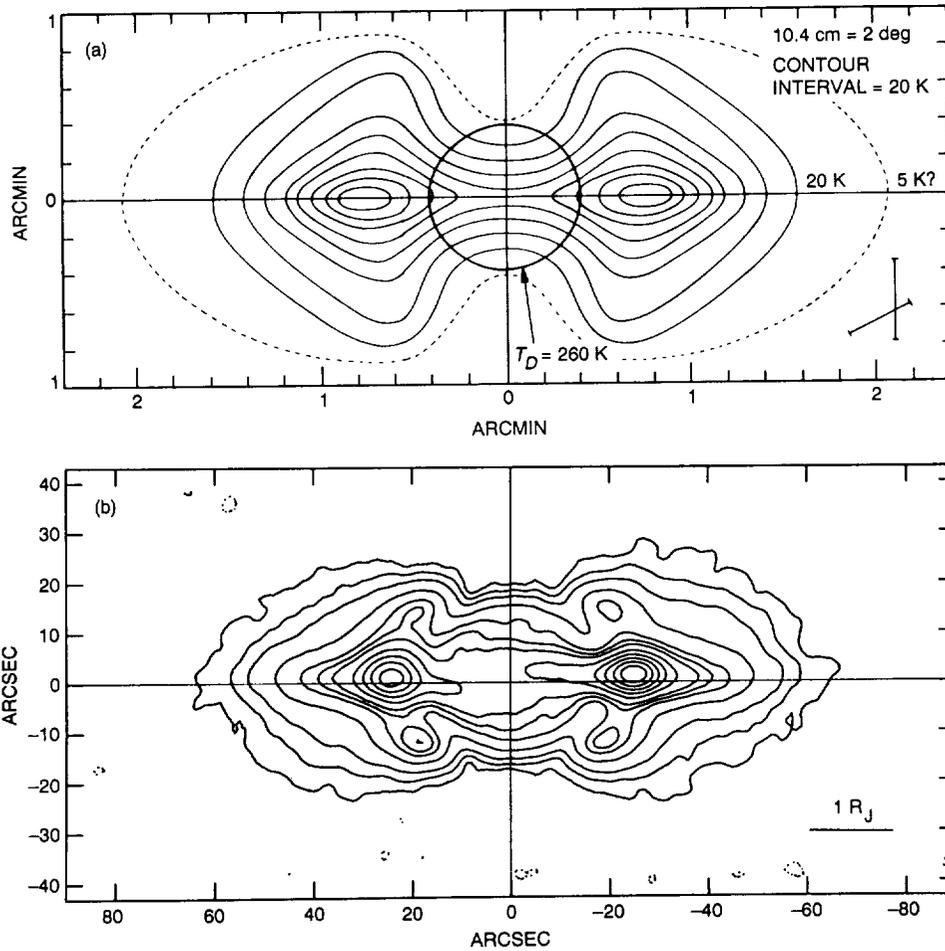
Fig. B-1. A map of the brightness distribution of Jupiter: (a) at 2.9 GHz with a 260-K disk component removed and 20-K contour intervals (from [6]) and (b) at 1.4 GHz, including disk component with contour intervals at 2, 5, 10, 20, 30, 35, 40, 50, 60, 70, 80, and 90 percent (from [7]).
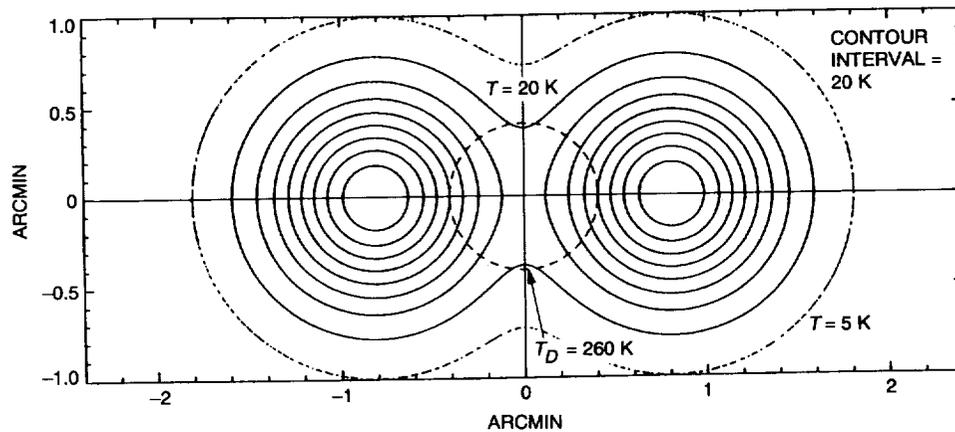

Fig. B-2. A model of Jupiter's brightness distribution at S-band [see Eq. (B-9)], plotted in the same format as Fig. B-1(a) with disk component removed.

Appendix C

Phasing

I. The Ideal Case

The SNR on the spacecraft is maximized when the terms in the double sum in Eq. (8) add in phase. This can be (approximately) arranged with the appropriate choice of model phases ϕ_i^m. By using Eq. (A-25), $\rho_{ik}^{s/c}$ will have zero phase for all i, k when

$$\delta\phi_k - \delta\phi_i = \phi_k - \phi_k^m - \phi_i + \phi_i^m = \frac{2\pi\nu_{sky}^{s/c}}{c}\mathbf{B}_{ik}\cdot(\hat{\mathbf{s}}_{s/c} - \hat{\mathbf{s}}_0)$$

(C-1)

The above relation can be satisfied if, for all $i = 1, ... N$,

$$\phi_i^m = \phi_i + \frac{2\pi\nu_{sky}^{s/c}}{c}\mathbf{B}_{ir}\cdot(\hat{\mathbf{s}}_{s/c} - \hat{\mathbf{s}}_0)$$

(C-2)

where r represents an arbitrarily chosen reference antenna.

The values of ϕ_i are not known a priori, but there are $N(N-1)/2$ independent measurements of the phase of the correlation function that can be used to fit for the N model phases ϕ_i^m (see [8]). Note that since $\delta\phi_i$, $\delta\phi_k$ include media effects as well as phase shifts in each antenna's signal path, they vary on timescales of seconds to minutes, so that the model phases must be recalculated at least that frequently to prevent degradation of the signal.

II. The Effects of Random Noise and a Background Planet

The above discussion ignores the contributions of random noise and a background planet to the observed phases. These complicate the process of solving for model phases, since what actually can be observed is the phase of the total correlation ρ_{ik}, not the phase of $\rho_{ik}^{s/c}$, the correlation due to the spacecraft signal.

The phase Φ_{ik}^ρ of the correlation function is given by

$$\tan\Phi_{ik}^\rho = \frac{\text{Im}(\rho_{ik})}{\text{Re}(\rho_{ik})}$$

$$= \frac{\text{Im}(\rho_{ik}^{s/c}) + \text{Im}(\rho_{ik}^P) + \text{Im}(\rho_{ik}^N)}{\text{Re}(\rho_{ik}^{s/c}) + \text{Re}(\rho_{ik}^P) + \text{Re}(\rho_{ik}^N)}$$

(C-3)

where Re and Im represent, respectively, the real and imaginary parts of the complex function. The simplest phasing algorithms make the approximation that the spacecraft signal is the dominant contribution to ρ_{ik}, i.e.,

$$\tan\Phi_{ik}^\rho = \frac{\text{Im}(\rho_{ik})}{\text{Re}(\rho_{ik})} \approx \frac{\text{Im}(\rho_{ik}^{s/c})}{\text{Re}(\rho_{ik}^{s/c})}$$

(C-4)

This approximation requires that $|\rho_{ik}^{s/c}| >> |\rho_{ik}^P|$ and $|\rho_{ik}^{s/c}| >> |\rho_{ik}^N|$ for all baselines $\mathbf{B}_{ik}$. Using Eqs. (A-24), (A-25), and (A-28), this implies

$$\mathcal{P}_{s/c} >> \frac{\Delta\nu S_P}{2}|\mathcal{F}_{ik}^P|$$

(C-5)

and

$$\mathcal{P}_{s/c} >> \frac{1}{2}\sqrt{\frac{T_i}{G_i}\frac{T_k}{G_k}}\sqrt{\frac{\Delta\nu}{T}}$$

(C-6)

In theory, the first of these conditions can be circumvented by modelling the contribution of ρ_{ik}^P to the phase of ρ_{ik} in the phasing algorithm. The second condition is more fundamental and can only be dealt with by decreasing the observing bandwidth (if the spacecraft is a narrowband source) or increasing the time over which the correlation is averaged.

Appendix D

Weighting Factors

The weighting factors W_i should be chosen so as to maximize β_ϕ, which is given by Eq. (15). Such W_i will satisfy the condition

$$\frac{d\beta_\phi}{dW_j} = 0 \tag{D-1}$$

for all $j = 1,...N$. Since one of the weighting factors can be chosen arbitrarily, this condition amounts to $N - 1$ equations for $N - 1$ variables.

If the effects of the planet can be ignored (i.e., $S_p \approx 0$), Eq. (15) reduces to

$$\beta_\phi = \frac{\left[\displaystyle\sum_{i=1}^{N} W_i^2 G_i + \sum_{i=1}^{N}\sum_{\substack{k \neq i}}^{N} W_i W_k \sqrt{G_i G_k} \right]}{\displaystyle\sum_{i=1}^{N} W_i^2 T_i} \tag{D-2}$$

and Eq. (D-1) becomes

$$\frac{d\beta_\phi}{dW_j} = 0 = \frac{\left[\displaystyle\sum_{i=1}^{N} W_i^2 T_i \right]\left[2W_j G_j + \sum_{k \neq j} W_k \sqrt{G_j G_k} \right] - 2W_j T_j \left[\displaystyle\sum_{i=1}^{N} W_i^2 G_i + \sum_{i=1}^{N}\sum_{k \neq i}^{N} W_i W_k \sqrt{G_i G_k} \right]}{\left[\displaystyle\sum_{i=1}^{N} W_i^2 T_i \right]^2} \tag{D-3}$$

It is not terribly difficult to show that this is satisfied for

$$W_i = \frac{\sqrt{G_i}}{T_i} \tag{D-4}$$

If the contribution of the planet to the system temperature at each antenna is accounted for, but the correlated noise terms are ignored, the optimal weighting is

$$W_i = \frac{\sqrt{G_i}}{T_i + G_i S_P} \tag{D-5}$$

This is appropriate for an extremely extended array. If correlated noise terms are included, it is difficult (perhaps impossible) to solve for W_i in closed form, but it can be done numerically. For the array configuration at the DSN complex in Australia, the weights obtained, including the effects of correlated noise, differ by only a few percent from those given by Eq. (D-5), and they have a negligible effect ($\lesssim 0.5$ percent) on the values of β_ϕ. In fact, though the values of W_i obtained, including the effects of correlated noise, often differ by ~ 10 percent from those obtained from Eq. (D-4), the resulting values of β_ϕ differ by $\lesssim 1$ percent. Therefore, throughout this article, Eq. (D-4) is used to calculate weighting factors.

References

[1] R. Stevens, "Applications of Telemetry Arraying in the DSN," *TDA Progress Report 42-72*, vol. October–December 1982, Jet Propulsion Laboratory, Pasadena, California, pp. 78–82, February 15, 1983.

[2] D. W. Brown, W. D. Brundage, J. S. Ulvestad, S. S. Kent, and K. P. Bartos, "Interagency Telemetry Arraying for Voyager–Neptune Encounter," *TDA Progress Report 42-102*, vol. April–June 1990, Jet Propulsion Laboratory, Pasadena, California, pp. 91–118, August 15, 1990.

[3] M. H. Brockman, "The Effect of Partial Coherence in Receiving System Noise Temperature on Array Gain for Telemetry and Radio Frequency Carrier Reception for Receiving Systems with Unequal Predetection Signal-to-Noise Ratios," *TDA Progress Report 42-72*, vol. October–December 1982, Jet Propulsion Laboratory, Pasadena, California, pp. 91–118, February 15, 1983.

[4] R. M. Hjellming, ed., *An Introduction to the NRAO Very Large National Radio Astronomy Observatory*, Socorro, New Mexico, 1983.

[5] W. N. Christiansen and J. A. Hogbom, *Radio Telescopes*, New York: Cambridge University Press, 1985.

[6] G. L. Berge and S. Gulkis, "Earth-Based Observations of Jupiter: Millimeter to Meter Wavelengths," in *Jupiter*, T. Geherls, ed., Tucson: University of Arizona Press, pp. 621–691, 1976.

[7] I. de Pater, "Radio Images of Jupiter's Synchrotron Radiation at 6, 20 and 90 cm," *Astronomical Journal*, vol. 102, pp. 795–805, August 1991.

[8] J. S. Ulvestad, "Phasing the Antennas of the Very Large Array for Reception of Telemetry From Voyager 2 at Neptune Encounter," *TDA Progress Report 42-94*, vol. April–June 1988, Jet Propulsion Laboratory, Pasadena, California, pp. 257–267, August 15, 1988.